

Capacity of Bosonic Communications

Jeffrey H. Shapiro^{*}, Vittorio Giovannetti[†], Saikat Guha^{*}, Seth Lloyd^{*}, Lorenzo Maccone^{**} and Brent J. Yen^{*}

^{*}*Massachusetts Institute of Technology, Research Laboratory of Electronics, Cambridge, MA 02139, USA*

[†]*NEST-INFN and Scuola Normale Superiore, Pisa, Italy*

^{**}*QUIT, Dipartimento di Fisica “A Volta”, Università di Pavia, Pavia Italy*

Abstract. The capacity C for transmitting classical information is investigated for Bosonic channels with isotropic Gaussian noise. For the pure-loss channel—in which signal photons may be lost in propagation—the exact value of C is derived. The Holevo information of this channel is shown to be additive, and a “classical” encoding procedure employing coherent states is shown to achieve capacity. For active channel models—in which noise photons are injected from an external environment or the signal is amplified with unavoidable quantum noise—upper and lower bounds are obtained for the capacity. These bounds are asymptotically tight at low and high noise levels. Exact capacity results—given by the lower bounds—would follow from proving the conjecture that a coherent-state input minimizes the output entropy from such channels.

INTRODUCTION

A principal goal of quantum information theory is evaluating the information capacities of important communication channels. At present, exact capacity results are known for only a handful of channels. Here we consider the classical capacity C of Bosonic channels with isotropic Gaussian noise. This study connects to a research line that began with the capacity derivation for the lossless (and hence noiseless) Bosonic channel [1, 2], and only very recently has yielded the capacity of the pure-loss Bosonic channel [3]. For that channel, we have the exact values of C for single-mode operation under an average photon-number constraint at the input, and for wideband operation under an average power constraint at the input. In both cases quantum entanglement is not necessary to achieve capacity, and “classical” encoding procedures employing coherent states suffice. This means that the Holevo information of the pure-loss channel is additive. Moreover, at high average powers we show that heterodyne detection is asymptotically optimum for single-mode operation and for far-field, free-space communication. For active channel models—in which noise photons are injected from an external environment or the signal is amplified with unavoidable quantum noise—we provide upper and lower bounds for the capacity, which are asymptotically tight at low and high noise levels. Exact results for these active channels would follow from proving the conjecture that a coherent-state input minimizes the output entropy from such channels [4].

CHANNEL MODELS

We are interested in the classical communication capacities of three Bosonic channels with isotropic Gaussian noise—the lossy channel, the amplifying channel, and the classical-noise channel—whose single-mode propagation characteristics are as follows. In each case the channel input is an electromagnetic-field mode with annihilation operator \hat{a} , and whose output is another field mode with annihilation operator \hat{a}' . Also, in each case, the associated wideband (multi-mode) descriptions of these channels can be built up from tensor-product constructions using the single-mode models. None of these channels constitute unitary evolutions, so they are all governed by trace-preserving completely-positive (TPCP) maps that relate their output density operators, $\hat{\rho}'$, to their input density operators, $\hat{\rho}$.

The TPCP map $\mathcal{E}_\eta^N(\cdot)$ for the single-mode lossy channel can be derived from the commutator-preserving beam splitter relation

$$\hat{a}' = \sqrt{\eta}\hat{a} + \sqrt{1-\eta}\hat{b}, \quad (1)$$

in which the annihilation operator \hat{b} is associated with an environmental (noise) mode, and $0 < \eta \leq 1$ is the channel transmissivity. For the pure-loss channel, the \hat{b} mode is in its vacuum state; for the thermal-noise channel this mode is in a thermal state, viz., an isotropic-Gaussian mixture of coherent states with average photon number $N > 0$,

$$\hat{\rho}_b = \int d^2\mu \frac{\exp(-|\mu|^2/N)}{\pi N} |\mu\rangle\langle\mu|. \quad (2)$$

The TPCP map $\mathcal{A}_\kappa^M(\cdot)$ for the single-mode amplifying channel can be derived from the commutator-preserving phase-insensitive amplifier relation

$$\hat{a}' = \sqrt{\kappa}\hat{a} + \sqrt{\kappa-1}\hat{c}^\dagger, \quad (3)$$

where \hat{c} is the modal annihilation operator for the noise introduced by the amplifier and $\kappa \geq 1$ is the amplifier gain. This amplifier injects the minimum possible noise when the \hat{c} -mode is in its vacuum state. We will also be concerned with the excess-noise case, in which the \hat{c} -mode's density operator is the isotropic-Gaussian coherent-state mixture,

$$\hat{\rho}_c = \int d^2\mu \frac{\exp(-|\mu|^2/N)}{\pi N} |\mu\rangle\langle\mu|, \quad (4)$$

with average photon number $N > 0$.

The classical-noise channel can be viewed as the cascade of a pure-loss channel \mathcal{E}_η^0 followed by a minimum-noise amplifying channel \mathcal{A}_κ^0 whose gain exactly compensates for the loss, $\kappa = 1/\eta$. Then, with $\eta = 1/(M+1)$, we obtain the following TPCP map for the classical-noise channel,

$$\hat{\rho}' = \mathcal{A}_M(\hat{\rho}) \equiv \int d^2\mu \frac{\exp(-|\mu|^2/M)}{\pi M} \hat{D}(\mu)\hat{\rho}\hat{D}^\dagger(\mu), \quad (5)$$

where $\hat{D}(\mu)$ is the displacement operator, i.e., $\hat{a}' = \hat{a} + m$ where m is a zero-mean, isotropic Gaussian noise with variance given by $\langle|m|^2\rangle = M$. This channel is especially interesting, because it is the quantum version of the additive white Gaussian noise channel whose capacity was defined and derived by Shannon.

CHANNEL CAPACITY

The classical capacity of a quantum channel is established by random coding arguments akin to those employed in classical information theory. A set of symbols $\{j\}$ is represented by a collection of input states $\{\hat{\rho}_j\}$ that are selected according to some prior distribution $\{p_j\}$. The output states $\{\hat{\rho}'_j\}$ are obtained by applying the channel's TPCP map $\mathcal{E}(\cdot)$ to these input symbols. The Holevo information associated with priors $\{p_j\}$ and states $\{\hat{\sigma}_j\}$ is given by,

$$\chi(p_j, \hat{\sigma}_j) = S\left(\sum_j p_j \hat{\sigma}_j\right) - \sum_j p_j S(\hat{\sigma}_j), \quad (6)$$

where $S(\hat{\sigma}) \equiv -\text{tr}(\hat{\sigma} \ln(\hat{\sigma}))$ is the von Neumann entropy. According to the Holevo-Schumacher-Westmoreland theorem [5], the capacity of this channel, in nats per use, is

$$C = \sup_n (C_n/n) = \sup_n \left\{ \max_{\{p_j, \hat{\rho}_j\}} [\chi(p_j, \mathcal{E}^{\otimes n}(\hat{\rho}_j))/n] \right\} \quad (7)$$

where C_n is the capacity achieved when coding is performed over n -channel-use symbols and the supremum over n is necessitated by the fact that channel capacity may be superadditive.

Lossless Channel

The lossless channel is governed by the TPCP map $\mathcal{E}_1^0(\cdot) = \mathcal{A}_1^0(\cdot)$. It has long been known [1, 2] that the capacity of the single-mode lossless channel—subject to a constraint \bar{N} on the transmitter's average photon number—is additive. It is achieved by random single-channel-use coding over number states using a Bose-Einstein prior, which yields

$$C = g(\bar{N}) \equiv (\bar{N} + 1) \ln(\bar{N} + 1) - \bar{N} \ln(\bar{N}), \text{ nats/use.} \quad (8)$$

Note that because the channel is lossless, transmission of the number state $|n\rangle$ implies reception of the same number state. Thus the probability of confusing distinct codewords is zero. Moreover, because the von Neumann entropy of a pure state is zero, we have that the preceding C expression represents the maximum von Neumann entropy of a single-mode field state whose average photon number is at most \bar{N} .

The capacity of the wideband lossless channel—in which all frequencies from zero to infinity are available, subject to a constraint P on the average transmitted power—is also known to be additive [1, 2]. It too is achieved by number-state encoding over single channel uses, this time with a multi-mode prior in which the photon numbers for different frequencies are independent Bose-Einstein variates whose mean values are optimized, via a Lagrange-multiplier technique, within the overall average power constraint. The resulting capacity is

$$C_{\text{WB}} = \sqrt{\frac{\pi P}{3\hbar}}, \text{ nats/sec.} \quad (9)$$

Recently [3], we have shown that the preceding single-mode and wideband capacities for the lossless channel can be achieved by coherent-state encoding over single channel uses. In the single-mode case the capacity-achieving prior is an isotropic Gaussian distribution; in the wideband case different frequencies are coded with independent, isotropic Gaussian priors whose variances are optimized within the overall average power constraint. Unlike the case for the number-state code ensemble that achieves capacity, there is a non-zero probability of confusing distinct finite-length codewords from this coherent-state ensemble. The proof that this coherent-state encoding can achieve the capacity of the lossless channel is an immediate consequence of our work on the pure-loss channel.

Pure-Loss Channel

Here we shall outline our derivation for the capacity of the single-mode, pure-loss channel; for the wideband case see [3]. The proof consists of comparing easily obtained lower and upper bounds on the capacity. Suppose we use coherent-state encoding over single channel uses. Then, because the coherent state $|\mu\rangle$ is transformed into the coherent state $|\sqrt{\eta}\mu\rangle$ by the TPCP map \mathcal{E}_η^0 , we have that

$$C \geq C_1 \geq \max_{p(\mu)} S\left(\int d\mu p(\mu) |\mu\rangle\langle\mu|\right) = g(\eta\bar{N}), \quad (10)$$

where the last equality is achieved by the isotropic Gaussian prior

$$p(\mu) = \exp(-|\mu|^2/\bar{N})/\pi\bar{N}, \quad (11)$$

because this makes the average input state a Bose-Einstein mixture of number states. On the other hand, any output state realized through the pure-loss channel \mathcal{E}_η^0 from an input state whose average photon number is at most \bar{N} can also be realized as the output state from the lossless channel \mathcal{E}_1^0 from an input state whose average photon number is at most $\eta\bar{N}$. This lossless channel can yield output states that cannot be obtained from the pure-loss channel, so

$$C(\eta, \bar{N}) \leq C(1, \eta\bar{N}) = g(\eta\bar{N}), \quad (12)$$

with the obvious notation for the capacity of a single-mode pure-loss channel as a function of its transmissivity and average photon number constraint. Thus we have coincident lower and upper bounds, and hence the capacity of the single-mode pure-loss channel has been determined.

It is interesting to compare the preceding single-mode and wideband capacities for the pure-loss channel with the corresponding capacities that are achieved when either optical homodyne or optical heterodyne reception is employed, instead of the optimum quantum measurement that is implicit in the Holevo information maximization. Here we find

$$C_{\text{hom}} = \ln(1 + 4\eta\bar{N})/2 \quad \text{and} \quad C_{\text{het}} = \ln(1 + \eta\bar{N}), \quad (13)$$

for the single-mode case, and

$$C_{\text{WB}} = \sqrt{\frac{\pi\eta P}{3\hbar}} = \frac{\pi}{\sqrt{3}} C_{\text{WB-hom}} = \frac{\pi}{\sqrt{3}} C_{\text{WB-het}}, \quad (14)$$

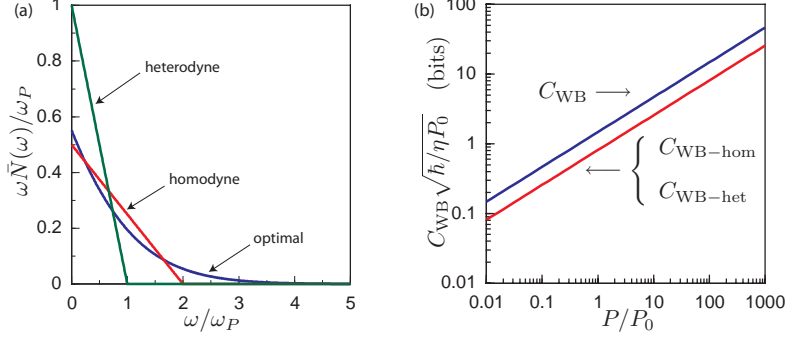


FIGURE 1. Capacity results for the pure-loss channel: (a) capacity-achieving power allocations $\hbar\omega\tilde{N}(\omega)$ versus frequency ω for heterodyne, homodyne, and optimal reception, with $\omega_P \equiv \sqrt{2P/\hbar}$ and $\hbar\omega_P$ being used to normalize the frequency and the power spectra axes, respectively; and (b) wideband capacities of optimal, homodyne, and heterodyne reception versus transmitter power P , with P_0 being an arbitrary reference power.

for the wideband case with frequency-independent loss, i.e., with η being a constant for $0 \leq \omega < \infty$. Equation (13) shows that single-mode homodyne detection outperforms single-mode heterodyne detection at low average photon numbers, and vice versa at high average photon numbers. These behaviors are easily understood. At low average photon numbers the noise advantage that homodyne detection enjoys in comparison with heterodyne detection is paramount, whereas at high average photon numbers it is heterodyne detection's bandwidth superiority that matters. More importantly, for the single-mode case, comparison of Eqs. (12) and (14) shows that $C_{het} \rightarrow C$ as $\tilde{N} \rightarrow \infty$. In contrast, Eq. (14) indicates that the wideband capacities of heterodyne and homodyne detection are identical, and both fall short of the capacity with optimum reception, see Fig. 1(b). This too is quite understandable. As shown in Fig. 1(a), the power allocations versus frequency for homodyne, heterodyne, and optimum transmission are all different. Evidently, the mix of high and low average photon numbers versus frequency for homodyne and heterodyne detection exactly balances their respective noise and bandwidth advantages. Likewise, the fact that both heterodyne detection and optimum reception have regions of low average photon number accounts for the gap between their respective capacities. For future reference, we note that Fig. 1(a) shows a preferential use of low frequencies for the wideband channel with frequency-independent loss. This occurs because high frequencies have more energetic photons that consume too much of the average power constraint to be heavily employed by capacity-achieving systems.

Although it serves as a useful illustrative example, wideband operation with frequency-independent loss is not a realistic scenario for the pure-loss channel. Thus we have also studied the far-field, free-space channel [3, 6], shown schematically in Fig. 2(a). Here, line-of-sight propagation occurs over an L -m-long path from a circular transmitter pupil (area A_t) to a circular receiver pupil (area A_r) with the transmitter restricted to use frequencies for $\{\omega : 0 \leq \omega \leq \omega_c \ll \omega_0 \equiv 2\pi cL/\sqrt{A_t A_r}\}$. This frequency range is the far-field power transfer regime, wherein there is only a single spatial mode that couples appreciable power from the transmitter pupil to the receiver pupil, and its transmissivity at frequency ω is $\eta(\omega) = (\omega/\omega_0)^2 \ll 1$. Figure 2(b) shows the power allocations versus frequency for heterodyne, homodyne, and optimal reception, and Fig. 2(c) plots the corresponding capacities versus normalized power, $P_0 \equiv 2\pi\hbar c^2 L^2/A_t A_r$. These figures contrast sharply with the results seen in Fig. 1 for the case of frequency-independent loss. In particular, because far-field, free-space transmissivity increases as ω^2 , high frequencies are used preferentially for this channel—unlike the case for frequency-independent loss—because the transmissivity advantage of high-frequency photons more than compensates for their higher energy consumption. Also, inasmuch as the Fig. 2 calculations apply to a channel with a finite available bandwidth ω_c , heterodyne detection is asymptotically optimal, because the average photon number used at all frequencies will become large as the transmitter power increases without bound.

Isotropic Gaussian-Noise Channels

For the thermal-noise, amplifying, and classical-noise channels, i.e., Bosonic channels with isotropic Gaussian noise, we have obtained bounds on the channel capacity. For the sake of brevity, we will restrict our discussion to the single-mode case. Lower bounds on single-mode capacities for these channels are easily obtained. We assume

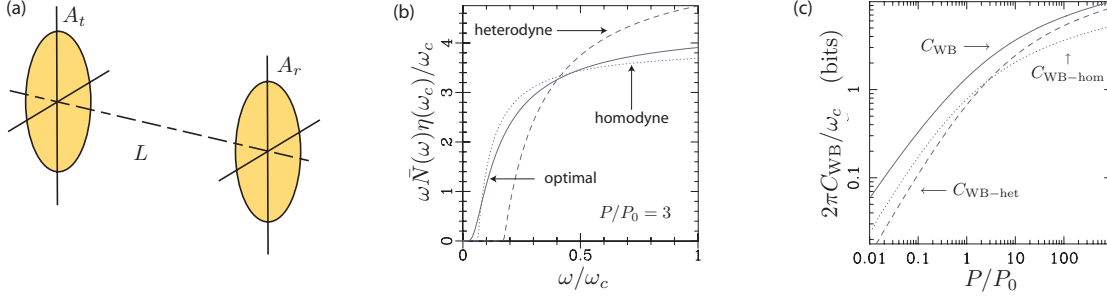


FIGURE 2. Capacity results for the far-field, free-space, pure-loss channel: (a) propagation geometry; (b) capacity-achieving power allocations $\hbar\omega\bar{N}(\omega)$ versus frequency ω for heterodyne, homodyne, and optimal reception, with ω_c and $\hbar\omega_c$ being used to normalize the frequency and the power spectra axes, respectively; and (c) wideband capacities of optimal, homodyne, and heterodyne reception versus transmitter power P , with $P_0 \equiv 2\pi\hbar c^2 L^2/A_t A_r$ used for the reference power.

coherent-state encoding over single channel uses with an isotropic Gaussian prior distribution. It then follows that

$$C \geq \begin{cases} g(\eta\bar{N} + (1-\eta)N) - g((1-\eta)N) & \text{thermal-noise channel,} \\ g(\kappa\bar{N} + (\kappa-1)(N+1)) - g((\kappa-1)(N+1)) & \text{amplifying channel,} \\ g(\bar{N} + M) - g(M) & \text{classical-noise channel.} \end{cases} \quad (15)$$

Corresponding upper bounds for the single-mode channel capacities can be connected to the problem of minimum output entropy by means of,

$$\begin{aligned} C_n/n &\leq \max_{\{p_j, \hat{\rho}_j\}} (S(\hat{\rho}')/n) - \min_{\hat{\rho}_j} (S(\hat{\rho}'_j)/n), \quad \text{where } \hat{\rho}' \equiv \sum_j p_j S(\hat{\rho}'_j) \\ &= \left. \begin{cases} g(\eta\bar{N} + (1-\eta)N) & \text{thermal-noise channel} \\ g(\kappa\bar{N} + (\kappa-1)(N+1)) & \text{amplifying channel} \\ g(\bar{N} + M) & \text{classical-noise channel} \end{cases} \right\} - \min_{\hat{\rho}_j} (S(\hat{\rho}'_j)/n) \end{aligned} \quad (17)$$

We believe that single-use coherent-state encoding with an isotropic Gaussian prior achieves channel capacity for the thermal-noise, amplifying, and classical-noise channels, i.e., we believe that the right-hand side of Eq. (15) gives the capacities of these channels. In support of our capacity conjecture, we have been working on the related conjecture that the minimum output entropy of these channels is obtained when their inputs are coherent states [4, 7]. Proof of the latter conjecture would, via Eqs. (15) and (17), complete the capacity proof. A sampling of our progress on the minimum output entropy conjecture is as follows. We have shown that a coherent-state input yields a *local* minimum of the output entropy. This local minimum then provides an upper bound on the global minimum, e.g., for a single use of the thermal-noise channel we have that

$$\mathbb{S}(\mathcal{E}_\eta^N) \equiv \min_{\hat{\rho}_j} \{S[\mathcal{E}_\eta^N(\hat{\rho}_j)]\} \leq g((1-\eta)N), \quad (18)$$

and for a single use of the classical-noise channel we find

$$\mathbb{S}(\mathcal{N}_M) \equiv \min_{\hat{\rho}_j} \{S[\mathcal{N}_M(\hat{\rho}_j)]\} \leq g(M). \quad (19)$$

We have also obtained a suite of lower bounds on the minimum output entropy, primarily for the single-use case and hence applicable to obtaining C_1 for isotropic Gaussian noise channels. These single-use bounds are illustrated in Figs. 3(a) and (b) for the thermal-noise and classical-noise channels, respectively—see [4] for details—along with the corresponding coherent-state-input upper bounds from Eqs. (18) and (19). As seen from these figures, for each of these channels our bounds provide fairly tight constraints on any possible gap between their minimum output entropy and the associated coherent-state upper bound on this quantity. Indeed these results imply that coherent-state encoding approaches the C_1 capacity at both low and high noise levels as seen from the $\eta \rightarrow 0$ and $\eta \rightarrow 1$ limits for the thermal-noise channel in Fig. 3(a) and the $M \rightarrow 0$ and $M \gg 1$ limits for the classical-noise channel in Fig. 3(b).

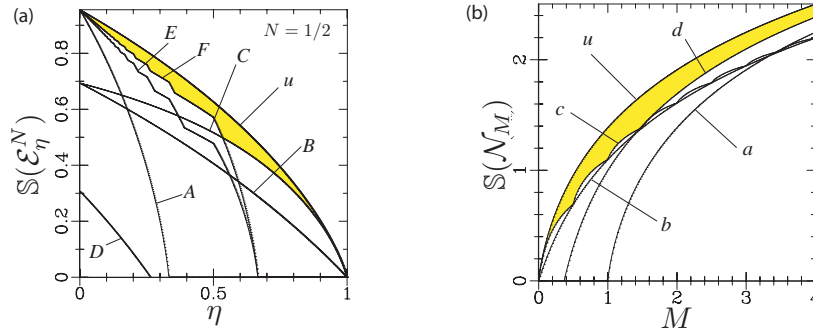


FIGURE 3. Bounds on the minimum output entropy for single-use Bosonic channels with isotropic Gaussian noise: (a) upper bound u and lower bounds A, B, C, D, E, F on the minimum output entropy $\mathbb{S}(\mathcal{E}_{\eta}^N)$ of the thermal-noise channel plotted versus channel transmissivity η for the case $N = 1/2$; and (b) upper bound u and lower bounds a, b, c, d on the minimum output entropy $\mathbb{S}(\mathcal{N}_M)$ of the classical-noise channel plotted versus the average photon number of the noise M . In both cases the upper bounds are the output entropies that result from coherent-state inputs. For details on the lower bounds see [4].

CONCLUSIONS

We have studied the classical capacity of a set of physically important Bosonic channels that are subject to isotropic Gaussian noise: the lossy channel, the amplifying channel, and the classical-noise channel. For the pure-loss channel we reported exact results for the capacity, showing that the Holevo information is additive for this channel and that capacity is achieved with a “classical” encoding procedure over coherent states. We also presented wideband capacities of pure-loss channels with frequency-independent and frequency-dependent (far-field, free-space propagation) loss. For the thermal-noise, amplifying, and classical-noise channels we obtained capacity lower bounds by assuming single-use encoding over coherent states. We conjecture that these lower bounds are in fact the channel capacities, and we presented evidence that is supportive of this conjecture.

ACKNOWLEDGMENTS

This work was supported by the DoD Multidisciplinary University Research Initiative (MURI) program administered by the Army Research Office under Grant DAAD19-00-0177.

REFERENCES

1. H. P. Yuen and M. Ozawa, Phys. Rev. Lett. **70**, 363 (1993).
2. C. M. Caves and P. D. Drummond, Rev. Mod. Phys. **66**, 481 (1994).
3. V. Giovannetti, S. Guha, S. Lloyd, L. Maccone, J. H. Shapiro, and H. P. Yuen, Phys. Rev. Lett. **92**, 027902 (2004).
4. V. Giovannetti, S. Guha, S. Lloyd, L. Maccone, and J. H. Shapiro, “Minimum output entropy of Bosonic channels: a conjecture,” to appear in Phys. Rev. A, e-print quant-ph/0404005.
5. A. S. Holevo, IEEE Trans. Inf. Theory **44**, 269 (1998); P. Hausladen, R. Jozsa, B. Schumacher, M. Westmoreland, and W. K. Wootters, Phys. Rev. A **54**, 1869 (1996); B. Schumacher and M. D. Westmoreland, Phys. Rev. A **56**, 131 (1997).
6. V. Giovannetti, S. Guha, S. Lloyd, L. Maccone, J. H. Shapiro, B. J. Yen, and H. P. Yuen, “Classical capacity of free-space optical communication,” in O. Hirota, ed. *Quantum Information, Statistics, and Probability* (Rinton Press, Princeton, 2004).
7. V. Giovannetti, S. Lloyd, L. Maccone, J. H. Shapiro, and B. J. Yen, Phys. Rev. A **70**, 022328 (2004).